
This is an electronic reprint of the original article.
This reprint may differ from the original in pagination and typographic detail.

Sahiluoma, Patrik; Yagodzinskyy, Yuriy; Forsström, Antti; Hänninen, Hannu; Bossuyt, Sven
Hydrogen embrittlement of nodular cast iron

Published in:
Materials and Corrosion : Werkstoffe und Korrosion

DOI:
[10.1002/maco.202011682](https://doi.org/10.1002/maco.202011682)

Published: 01/01/2021

Document Version
Publisher's PDF, also known as Version of record

Published under the following license:
CC BY

Please cite the original version:
Sahiluoma, P., Yagodzinskyy, Y., Forsström, A., Hänninen, H., & Bossuyt, S. (2021). Hydrogen embrittlement of nodular cast iron. *Materials and Corrosion : Werkstoffe und Korrosion*, 72(1-2), 245-254.
<https://doi.org/10.1002/maco.202011682>

This material is protected by copyright and other intellectual property rights, and duplication or sale of all or part of any of the repository collections is not permitted, except that material may be duplicated by you for your research use or educational purposes in electronic or print form. You must obtain permission for any other use. Electronic or print copies may not be offered, whether for sale or otherwise to anyone who is not an authorised user.



Hydrogen embrittlement of nodular cast iron

Patrik Sahiluoma | Yuriy Yagodzinsky | Antti Forsström |
Hannu Hänninen | Sven Bossuyt

Department of Mechanical Engineering,
Aalto University School of Engineering,
Aalto, Finland

Correspondence

Patrik Sahiluoma, Department of
Mechanical Engineering, Aalto University
School of Engineering, PO Box 14200,
FI-00076 Aalto, Finland.

Email: patrik.sahiluoma@aalto.fi

Funding information

KYT2022 (Finnish Research Program on
Nuclear Waste Management)

Abstract

Ferritic nodular cast iron, intended for use as the material for inserts of canisters for long-term geological disposal of spent nuclear fuel, was studied for hydrogen sensitivity. In the canisters, the insert provides the mechanical strength against external loads. Hydrogen was charged from 0.1 N H₂SO₄ solution in free-corrosion tests and under controlled cathodic potential. Hydrogen uptake and trapping were then measured using thermal desorption spectroscopy. The hydrogen desorption rate after hydrogen charging manifests two distinct peaks. Plastic deformation during hydrogen charging increases the hydrogen uptake considerably. Hydrogen reduces the elongation to fracture and time to fracture in slow strain rate testing and constant load testing (CLT), respectively. Especially, the strain rate in CLT is dramatically increased. The appearance of hydrogen-induced cracking in the ferrite phase changes from ductile dimple fracture to brittle cleavage fracture due to hydrogen charging, which initiates from the interphases of the graphite nodules. The results are discussed in terms of the role of hydrogen and the graphite nodules in hydrogen embrittlement of ductile cast iron.

KEYWORDS

copper canister, ductile cast iron, hydrogen embrittlement, hydrogen thermal desorption, hydrogen trapping, spent nuclear fuel

1 | INTRODUCTION

In the KBS-3 method of long-term geological disposal of spent nuclear fuel, the load-bearing inserts of the canisters are intended to be manufactured from ferritic nodular ductile cast iron (DCI) EN 1563 grade EN-GJS-400-15U^[1–3] (Figure 1). Recent studies of hydrogen effects on the mechanical performance of DCI have shown a remarkable sensitivity to hydrogen in the form of hydrogen embrittlement and hydrogen-enhanced creep.^[4] There are some possible internal sources of hydrogen in the canister

in addition to the metallurgical hydrogen originating from manufacturing: residual water from the spent nuclear fuel assemblies, the amount of which left in each canister in accordance with the design case must be <600 g,^[1,3] and hydrogen produced by (n, p) reactions and hydrides formed in the zirconium–alloy fuel assemblies.^[5] The effects of hydrogen on all canister materials, including DCI, have to be known and taken into account in the safety analysis of spent nuclear fuel disposal.

The DCI's mechanical properties are affected by the microstructure of its matrix (ferrite and possibly some

This is an open access article under the terms of the Creative Commons Attribution License, which permits use, distribution and reproduction in any medium, provided the original work is properly cited.

© 2020 The Authors. *Materials and Corrosion* published by Wiley-VCH Verlag GmbH & Co. KGaA



FIGURE 1 KBS-3 canister. Copper shell and lid on the left and cast iron insert and steel lid of the insert on the right. Posiva Oy [Color figure can be viewed at wileyonlinelibrary.com]

pearlite) together with the shape, size, and distribution of graphite, slag inclusions, porosity, and casting defects.^[6–8] The requirements for the mechanical properties of the insert material, ferritic nodular cast iron, are at ambient temperature: elongation to fracture >12%, tensile yield strength >240 MPa, ultimate tensile strength >370 MPa, and fracture toughness (in ductile fracture) $K_{Ic} > 78 \text{ MPa(m)}^{1/2}$.^[1–3]

The effects of hydrogen on the embrittlement of various nodular cast irons have been reported in several studies.^[4,9–12] The studies show that the available hydrogen tends to accumulate in the graphite nodules and on the graphite/matrix interfaces.^[9,12] Under the influence of hydrogen, this material with typically ductile behavior shows a cleavage-like brittle fracture in the ferrite matrix between graphite nodules. This is observed, in particular, under slow strain rates.^[4,11,12]

To investigate the hydrogen embrittlement of DCI, the microstructure was examined in the as-supplied state and after charging to understand the changes caused by hydrogen on the microstructure. Then, the samples were studied with hydrogen thermal desorption spectroscopy (TDS) and scanning electron microscopy (SEM) after free-corrosion immersion, electrochemical hydrogen charging, and after slow strain rate tensile testing (SSRT), and constant load testing (CLT) under continuous hydrogen charging.

2 | EXPERIMENTAL METHODS

The effects of hydrogen on the graphite morphology and mechanical performance of ferritic nodular cast iron grade EN-GJS-400-15U were studied. The chemical composition of the studied DCI is shown in Table 1. Casting I73 produced by Posiva Oy, Finland, was cut as shown in Figure 2. A block of the material was cut from the location marked with red

square (B) for manufacturing the specimens for tensile testing and hydrogen charging. The samples were cut from near the surface of the casting and from the depth of ~40 mm, using electro-discharge machining (EDM). Two types of specimens were made, that is, tensile specimens according to the geometry shown in Figure 2b and TDS samples shown in Figure 2c. Both specimens were mechanically ground to remove the EDM-affected surface layer. The gauge section of the tensile specimens was mechanically polished, finishing with 2,500 grit emery paper without lubrication. The TDS samples were polished up to 2,500 grit emery paper using common wet grinding and polishing techniques. After CLTs, the TDS samples were cut immediately after terminating the tensile test from the gauge part of the tensile specimens and polished using the emery papers.

The tensile specimens were studied with SSRT and CLT in air and under continuous hydrogen charging with controlled electrochemical potential. The testing system consists of a 35 kN MTS desktop tensile testing machine equipped with a three-electrode electrochemical cell with Hg/Hg₂SO₄ reference and Pt counter electrodes and a Gamry potentiostat for controlled hydrogen charging. The test set-up is shown in Figure 3. Electrochemical hydrogen charging was performed at a controlled cathodic potential of –0.85 V from 0.1 N H₂SO₄ solution with added 10 mg/L thiourea. Each hydrogen charged tensile test was preceded by 1 hr precharging to uniformly saturate the specimen with hydrogen before loading. Only the gauge parts of the tensile specimens were exposed to the environment by insulating the rest of the immersed specimen with polytetrafluoroethylene (PTFE) tape. The total volume of the solution was about 1,600 cm³ and the pumping rate was 2 cm³/s circulating between the test cell and the conditioning container, which held the extra solution.

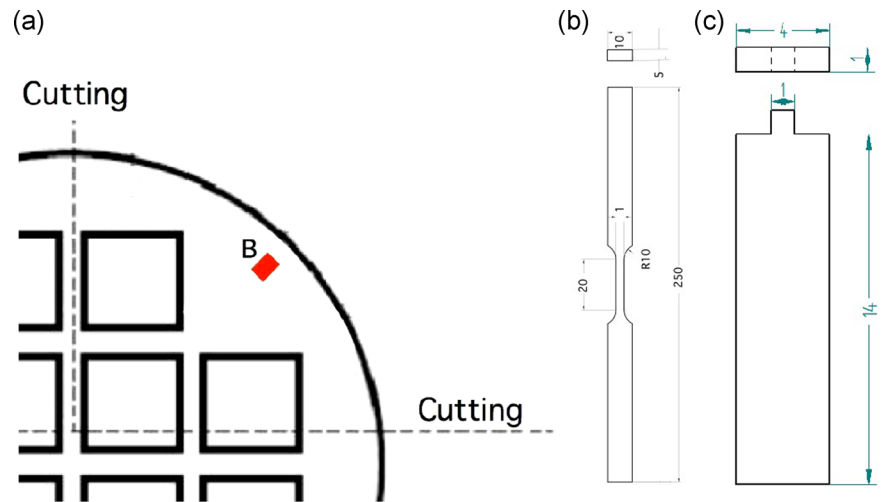
The SSRTs were performed with the strain rate of 10^{–4} s^{–1}. The CLTs were performed in two stages: preloading with 10^{–4} s^{–1} strain rate up to load of 160 MPa (about 0.5 tensile strength of the studied DCI) as in the previous study.^[4] After preloading, the load was kept constant for a predetermined time or until fracture. The hydrogen uptake of the material was then immediately measured by using TDS. The time between termination of the hydrogen charging and starting the TDS measurement was kept to a minimum and did not exceed 20 min.

The TDS samples were exposed to the environment in two ways. First, they were simply submerged in 0.1 N

TABLE 1 Chemical composition of nodular cast iron EN-GJS-400-15U (insert I73) in wt%

C	Si	Mn	S	P	Ni	Cu	Mg	Fe
3.48	2.48	0.22	0.004	0.01	0.04	0.02	0.04	Bulk

FIGURE 2 (a) The location of billet from which the samples were cut, marked with B, (b) tensile specimen geometry, and (c) thermal desorption spectroscopy sample geometry [Color figure can be viewed at wileyonlinelibrary.com]



H_2SO_4 solution with added 10 mg/L thiourea being attached to a PTFE wrapped wire to study hydrogen absorption in the sample without external electrochemical polarization. Second, the samples were exposed in a similar three-electrode system with electrochemical potential control at -0.85 V in a similar chamber to the one used for tensile testing, but without mechanical loading.

Hydrogen uptake and trapping were measured using a custom-made TDS apparatus designed and assembled at Aalto University. The device is based on the mass spectrometry of hydrogen desorption in an ultra-high vacuum

chamber under a constant controlled heating rate. With a vacuum of 5×10^{-9} mbar, the hydrogen concentration measurements are accurate down to quantities of about 0.1 at ppm. The equipment allows the heating rate to be varied between 1 and 10 K/min allowing the evaluation of the activation energy of the hydrogen trapping sites in the studied material. The operating temperature range is from room temperature (RT) to $1,200^\circ\text{C}$. The heating rate of 10 K/min was used from RT to 650°C to study the release of hydrogen and the behavior of trapping sites in DCI. The Kissinger procedure^[13,14] was utilized with different heating rates to evaluate the hydrogen trapping energies of different sites.

The microstructural analysis and fractography were performed with a Zeiss Ultra 55 field emission gun scanning electron microscope. When applicable, the SEM specimens were mounted using Struers PolyFast resin and were prepared using conventional wet grinding and polishing techniques down to a $0.25\text{-}\mu\text{m}$ diamond paste.



FIGURE 3 The tensile testing system consisting of a 35 kN MTS desktop machine with an electrochemical cell and Gamry potentiostat [Color figure can be viewed at wileyonlinelibrary.com]

3 | RESULTS

3.1 | Hydrogen effects on SSRT and CLT of cast iron

Typical stress–strain curves obtained in SSRT are shown in Figure 4 and strain versus time plots obtained in CLT in Figure 5. As in the previous study,^[4] the DCI's mechanical properties show a remarkable reduction under hydrogen charging. The ultimate tensile strength of the material was markedly reduced in the SSRT test under hydrogen charging and the elongation to fracture was halved.

The behavior of the DCI was more closely examined using CLTs (Figure 5). Most CLT tests were interrupted before failure to study the evolution of the material's

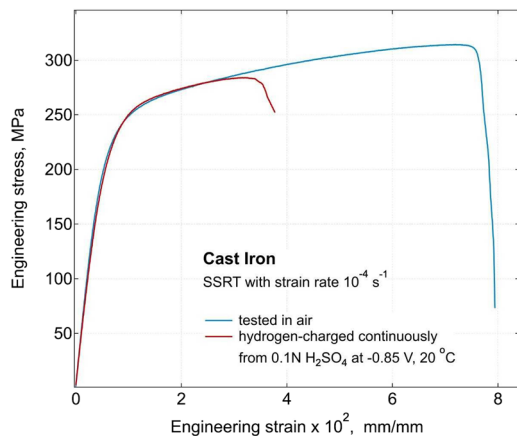


FIGURE 4 Slow strain rate tensile testing (SSRT) stress–strain curves in the air (blue) and under continuous hydrogen charging (red) tested at room temperature [Color figure can be viewed at wileyonlinelibrary.com]

deformation and crack initiation in constant loading under hydrogen charging by examining the changes in the graphite nodules and ferrite matrix of the material. When the specimen was kept at a constant applied stress of 160 MPa in air, the specimen did not show any remarkable creep strain during the test period of several days. However, when repeating the test under continuous hydrogen charging, the specimen elongated at an accelerating rate leading to eventual fracture. There was a noticeable scatter in the strain rates of different tests. The scatter is, however, understandable due to several factors: the comparatively small gauge size of the tensile specimens means that the effects of any discontinuities in the microstructure are enhanced. In other words, the fraction and size of graphite nodules in relation to the size of the cross-section of the specimen and their location with respect to the edges of the specimen bring random variations to the experiment. For instance, if a graphite nodule is located at or close to the edge of the specimen, it causes stress concentration at the edge, leading possibly to cracking in that location.

3.2 | Hydrogen uptake and trapping

The temperature position of the hydrogen desorption peak depends on the effective trapping site of hydrogen, as well as on the heating rate of the sample. The magnitude and shape of the peak are related to hydrogen release in each of the trapping sites. Thus, the area under the peaks corresponds with the amount of hydrogen trapped at these sites.

The as-supplied state of the material was studied previously and it was found that the studied DCI showed

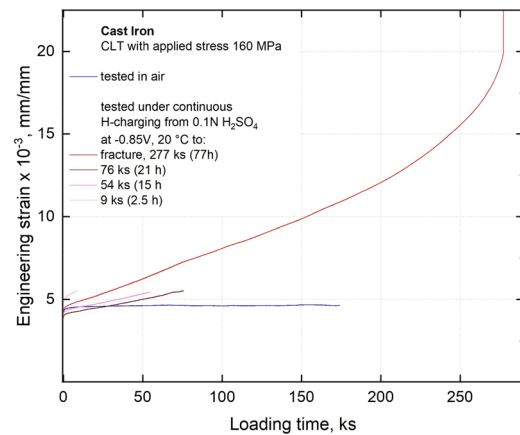


FIGURE 5 Strain versus time curves in constant load testing (CLT) in the air (blue) and under continuous hydrogen charging (shades of red) tested at room temperature [Color figure can be viewed at wileyonlinelibrary.com]

two peaks, one around 500 K and the other one at 700 K.^[4] These peaks correspond with the existing metallurgical hydrogen of about 2 wt ppm in the studied DCI. In tensile loading, a peak appeared at about 400 K and the 500 K peak shifted closer to 560 K with a large increase in its magnitude under electrochemical hydrogen charging. The magnitude of the 400 K peak also markedly increased and the location shifted towards 450 K in tensile testing with hydrogen charging.^[4]

In this study, the DCI shows two distinct peaks of hydrogen thermal desorption. Figure 6a shows the hydrogen desorption peaks when the sample is immersed freely in 0.1 N H₂SO₄ solution without external mechanical loading or applied electrochemical potential. The immersion time affects significantly the location and magnitude of the peak correlating with the amount of trapped hydrogen in the sample. The TDS curve for immersion time of 2,400 s (40 min), for instance, shows how hydrogen absorption mostly manifests as a 600 K peak. The longer immersion times result in the saturation of this high-temperature peak, the desorption rate being about 0.4 at ppm/s. As the immersion time is increased, the magnitude of the low-temperature peak at 450 K keeps increasing. This means that an increasing amount of hydrogen is being trapped in this trapping site.

Figure 6b shows similar behavior to the free-immersion tests for the specimens tested with the external electrochemical potential control for hydrogen charging. The high-temperature peak reaches a similar saturation level of 0.4 at ppm/s, after which the low-temperature trapping site is gradually activated. The amount of trapped hydrogen increases with charging time, reaching a similar level as in the free-immersion tests. With the introduction of the external

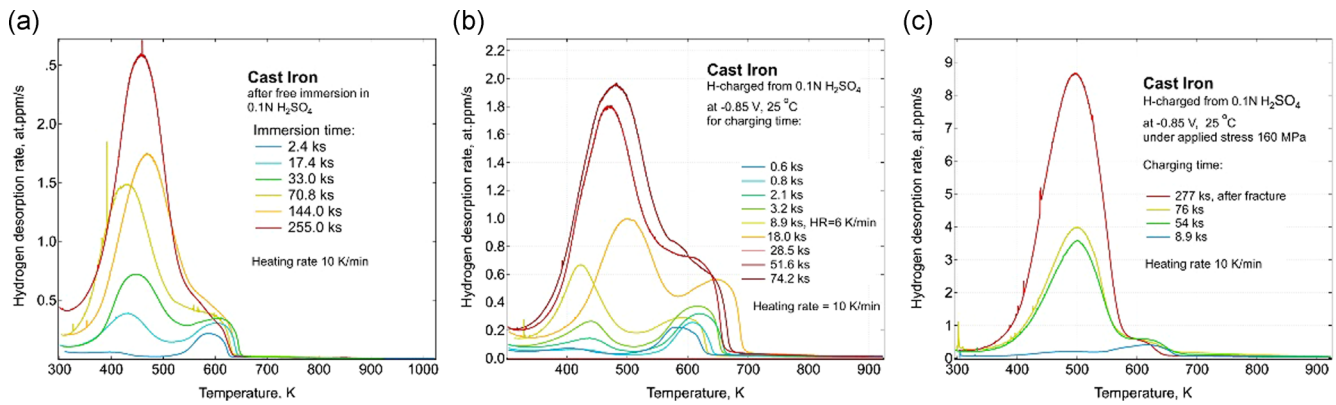


FIGURE 6 The characteristic peaks of hydrogen desorption from ductile cast iron in different test conditions. (a) After free immersion in 0.1 N H₂SO₄ solution for different immersion times. (b) After electrochemical hydrogen charging for different times. (c) Measured from the gauge section of constant load testing specimens after interrupted testing under electrochemical charging [Color figure can be viewed at wileyonlinelibrary.com]

electrochemical potential control, the time necessary to absorb the same amount of hydrogen is, however, reduced markedly.

Figure 6c shows TDS curves obtained after CLTs under continuous hydrogen charging. Again, the high-temperature peak is saturated and the low-temperature peak gradually increases. However, now under both tensile loading and electrochemical hydrogen charging, the low-temperature peak increases markedly more as compared to the unloaded conditions. Thus, it can be concluded that an external tensile loading causes the formation of effective trapping sites which are responsible for the increase of hydrogen uptake.

Assuming that the desorption peaks can be approximated with Gaussian functions, the measured complex TDS peaks were decomposed into two components as shown in Figure 7a. Applying the decomposition procedure to the TDS peaks measured for the samples with different electrochemical charging times, one can obtain dependencies of the hydrogen concentration

corresponding to each component versus charging time as shown in Figure 7b. As the charging time increases, the amount of hydrogen corresponding to the high-temperature peak remains the same, but it increases with time for the low-temperature peak. The closed nature of these peaks is examined more closely in Section 4. Using the Kissinger procedure^[13,14] for activation analysis of both peak temperature positions versus the heating rate of TDS measurement as shown in Figure 7c, the trapping energy for these peaks can be found to be 0.30 ± 0.006 and 0.65 ± 0.03 eV, most likely corresponding with the ferrite matrix and the graphite nodules, respectively.

3.3 | Microstructure and fractography of DCI with hydrogen

Typical microstructures of the studied DCI are shown in Figure 8. The material consists of a ferritic matrix with dispersed graphite nodules. The graphite is mostly

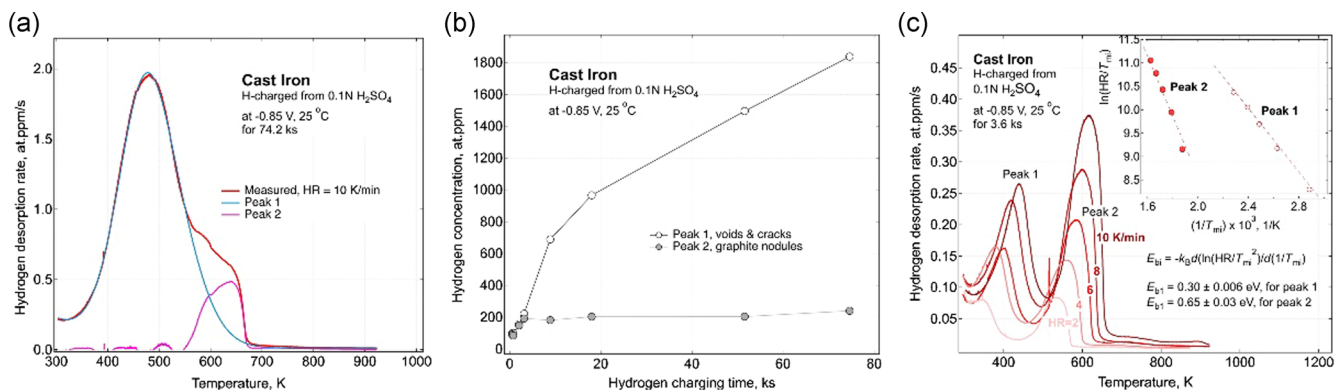


FIGURE 7 The characteristics of thermal desorption spectroscopy (TDS) curves. (a) The decomposition of measured TDS curve into two peaks, (b) the amount of trapped hydrogen as a function of electrochemical charging time, and (c) activation analysis for both components of the peak [Color figure can be viewed at wileyonlinelibrary.com]

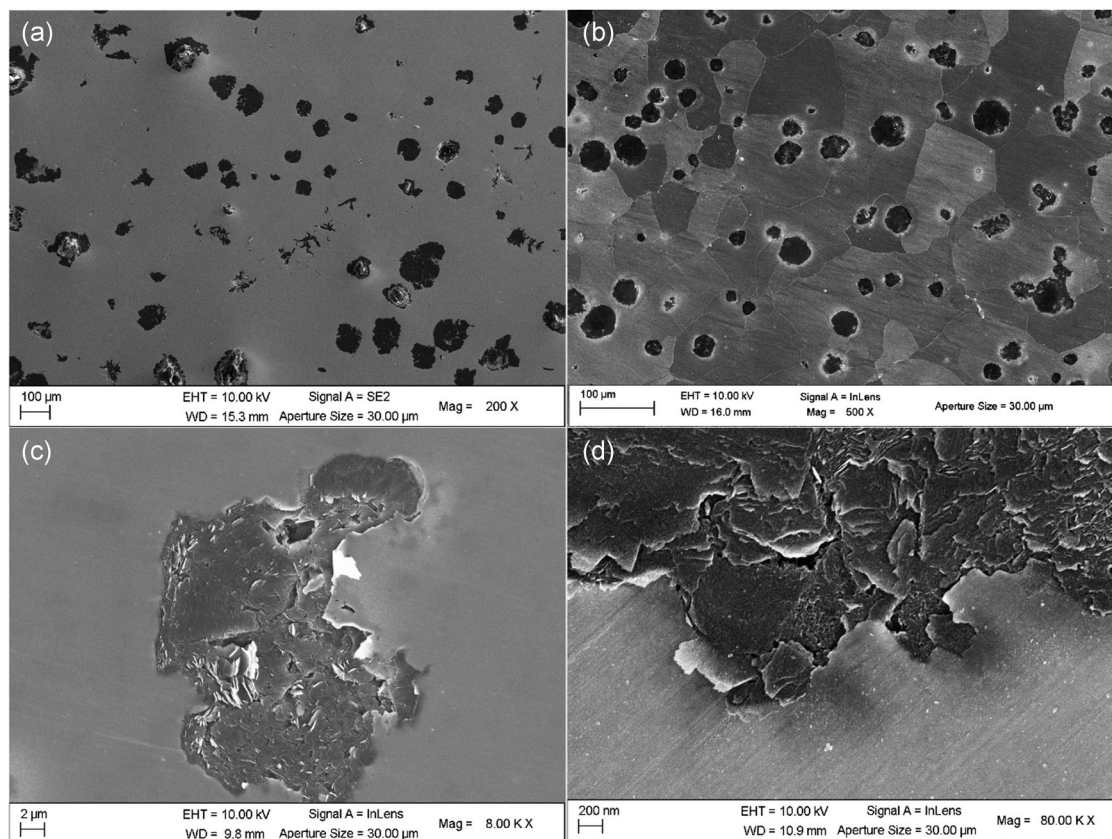


FIGURE 8 (a) General view of microstructure of as-received ductile cast iron cut from near casting surface and (b) after etching in 2% nital solution. (c) A graphite nodule and (d) the graphite nodule/ferrite matrix interface before hydrogen charging

nodular with somewhat uneven distribution of nodules related most likely to the segregation of alloying elements during solidification. All nodules are of type V and type VI according to EN ISO-945-1:2018. The volume fraction of the graphite nodules is about 0.056. The average nodule size in the studied part of the cast iron insert is about $44.5 \mu\text{m}$, and the volume density of the graphite nodules is $6.31 \times 10^{12} \text{m}^{-3}$. The spheroidal graphite nodules have a layered flaked structure and incoherent graphite/ferrite interface (Figure 8c,d). The grain size of the ferrite matrix is about $78 \mu\text{m}$ and a very small amount of pearlite is present (<5%).

The graphite nodules are affected by hydrogen charging (Figure 9a), and especially, the graphite nodule/ferrite matrix interfaces exhibit multiple small cracks in the ferrite matrix formed under hydrogen charging (Figure 9b–d). Cracking at the interface of the graphite nodules and eventual linkage of cracking between the graphite nodules was not observed in the as-supplied DCI (Figure 8). Only under hydrogen charging and with increasing charging time or introduction of tensile loading, microcracking at graphite nodule/ferrite matrix interfaces appears in increasing numbers, and the cracks grow and connect forming a series of larger step-wise brittle cracks in the material.

The fracture surface of an SSRT specimen tested in the air is shown in Figure 10. It exhibits the typical ductile fracture characteristics in the form of large cavities around the graphite nodules and small dimples in the ligaments, as is expected of the DCI tested in the air (elongation to fracture 8%). With the uptake of hydrogen under constant load, however, the ligaments between the large cavities show brittle cleavage fracture facets as shown in Figure 11a,b. The cleavage fracture occurs in the ferrite between the graphite nodules. Large cavities are also left by the graphite nodules in the ferrite matrix. In the large cavities, the interface between the graphite nodules and the ferrite matrix becomes visible showing a faceted surface structure (Figure 11c,d). Energy-dispersive X-ray spectroscopy analysis of the faceted cavity surfaces shows only the presence of iron in the spectrum indicating an interfacial detachment of the graphite nodules during tensile testing.

4 | DISCUSSION

The TDS results show that the hydrogen uptake in free-immersion and electrochemically charged DCI samples are similar, but the electrochemically charged samples

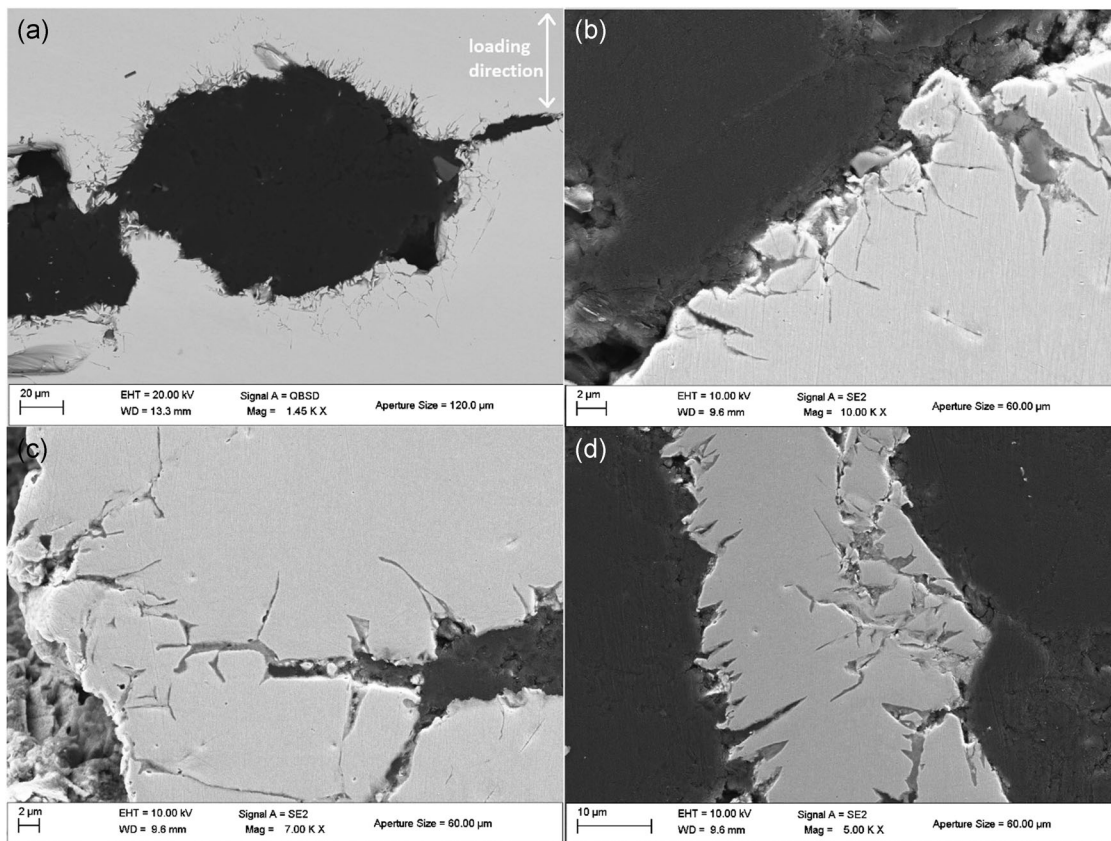


FIGURE 9 Graphite nodules of constant load testing tensile specimen cut from location B. Tested up to fracture (loading time 238 ks/66 hr). (a) The general appearance of cracking around a nodule, (b) close-up of cracking at nodule/matrix interface, and (c and d) linking between adjacent graphite nodules by brittle cleavage cracking

show uptake of hydrogen at a much higher rate. The behavior of the material in free-immersion tests shows that the microstructure of DCI affects the uptake of hydrogen autocatalytically when hydrogen is available. This means that the DCI in free-immersion forms microgalvanic couples between the iron matrix and the

graphite nodules where the graphite nodules act as local cathodes and the iron matrix is the anode.

By comparing the TDS curves of the different testing conditions, it can be concluded that the high-temperature peak (600 K) of hydrogen desorption depends only slightly on the hydrogen charging method and external

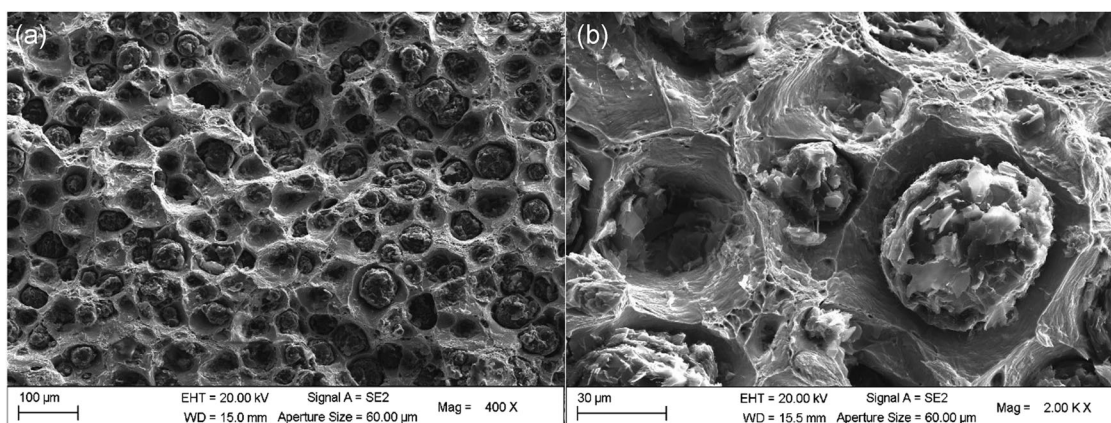


FIGURE 10 The fracture surface of slow strain rate tensile testing specimen loaded in the air showing ductile fracture with large cavities around graphite nodules and small dimples in ferrite ligaments

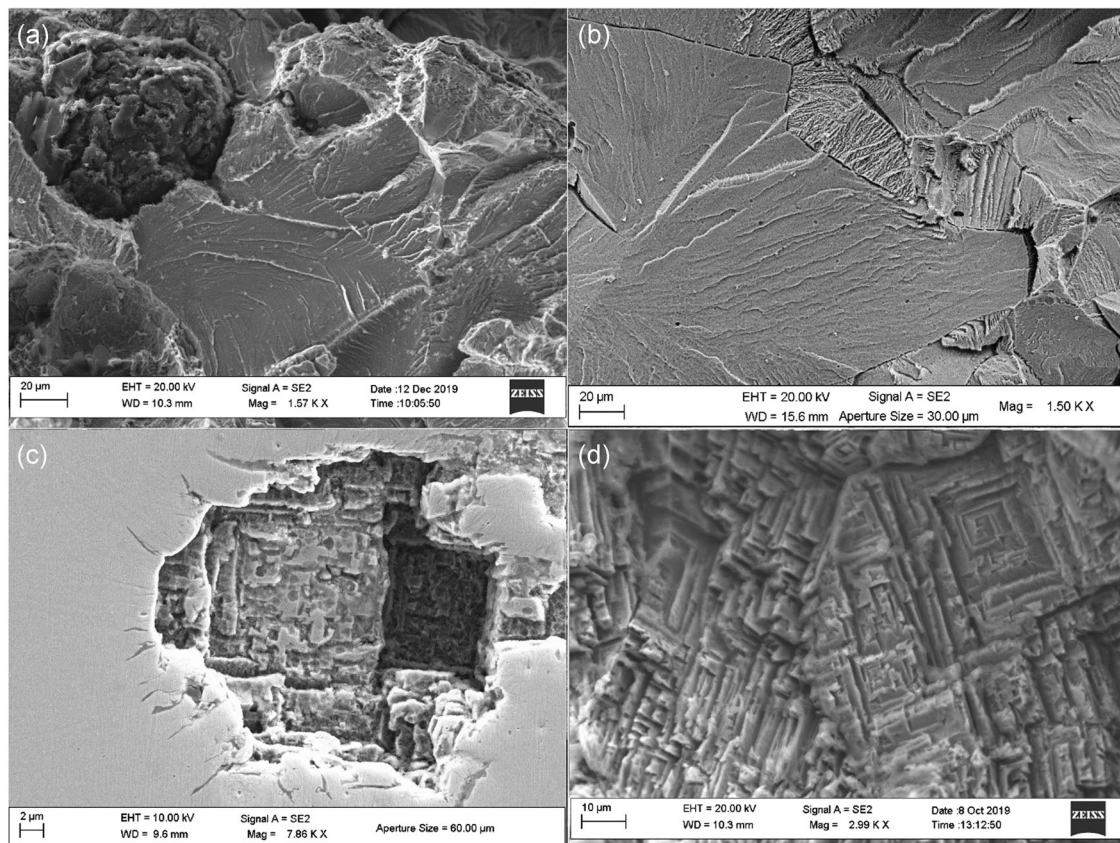


FIGURE 11 Hydrogen charged constant load testing specimens. (a) General view of the fracture surface and (b) a close-up of brittle cleavage fracture facets in ferrite ligaments. (c) Side view of polished specimen cross-section surface showing multiple small brittle cracks around a cavity left by a detached graphite nodule and (d) a close-up of the surface of the cavity

loading, and it will reach a saturation level of hydrogen content. This indicates that the high-temperature peak is related to a trapping site that does not markedly change due to the charging procedure. Assuming that the graphite nodules have a limited capacity to absorb hydrogen and that the amount of graphite nodules in the material is the same in different samples, it may be concluded that the high-temperature peak is related to hydrogen trapped in the graphite nodules. The low-temperature peak (450 K), however, is highly dependent on the external loading of the specimen.

When the graphite morphology and microstructure of the DCI were examined before and after hydrogen charging, it was observed that the presence of hydrogen causes the initiation of multiple small cracks around some graphite nodules. The number of cracks and severity of cracking was observed to increase with the increasing charging or immersion time and especially due to tensile loading. With long enough hydrogen charging time or at high enough applied stress in CLT, the small cracks link between the graphite nodules leading to crack growth and consequent hydrogen trapping in the small

cracks. The hydrogen-induced cracks and defects at the graphite nodule interfaces are, thus, assumed to be the reason for the increasing hydrogen uptake related to the growing low-temperature peak.

The micrographs of CLT specimens revealed that the presence of hydrogen causes multiple small cracks to initiate from the nodule interfaces around the graphite nodules. In all conditions where hydrogen was available to the specimens (immersion with or without electrochemical potential control and during tensile loading), the graphite nodules show initiating small cracks at their interfaces. With increasing time and the introduction of an external tensile load, the small cracks coalesce between graphite nodules causing large cracks in the microstructure.

The CLT and SSRT tests show that under continuous hydrogen charging the mechanical properties of DCI are markedly reduced compared with performance in the air showing similar behavior as in the previous study.^[4] Fractography after CLT shows the separation of graphite nodules from the ferrite matrix with the faceted interface of the cavities and cleavage fracture in ferrite between the

graphite nodules (Figure 11a,b). In the air without hydrogen (Figure 10), ductile fracture occurs forming small dimples in the ferrite ligaments typical for a ductile material such as DCI. It is of great significance that the fracture behavior of DCI changes markedly in the presence of hydrogen. Hydrogen diffuses freely through ferrite, but the graphite nodules can uptake the available hydrogen and become saturated. The hydrogen build-up and resulting internal gas pressure may eventually cause the graphite nodules to detach from the ferrite matrix. This introduces cracks in the microstructure and leads to the initiation of brittle cleavage fracture.

The graphite nodules show multiple cracking around their interface. These small cracks increase in number and size as samples are charged for longer periods of time or with applied external tensile loading. The reason for the initiation of multiple cracks at the graphite/ferrite matrix interfaces is related to hydrogen behavior in DCI. Metallurgical hydrogen (about 2 wt ppm) builds up in austenite during solidification and during decomposition of austenite upon cooling graphite nodules in the DCI act as trapping sites for hydrogen. Graphite nodules exhibit decohesion at the interface between the graphite and ferrite matrix (Figure 8). Decohesion can have occurred before hydrogen charging as graphite nodules have a weak interface with the ferrite matrix. Hydrogen trapping and recombination to hydrogen gas at the graphite nodule/ferrite matrix interfaces forms hydrogen gas molecules, creating an internal pressure. Hydrogen-induced cracking then results from the formation of high-pressure gas in the internal cavities and microcracks.^[15] Graphite nodules are the preferable hydrogen-induced crack initiation sites creating internal cracks. The pressure build-up in the internal cracks due to hydrogen recombination results in the crack growth. The critical hydrogen concentration at the graphite nodule interfaces is not known, but the crack initiation took place at graphite nodules independently of the charging conditions. The faceted interface (Figure 11c,d) between graphite nodules and ferrite matrix with geometrical discontinuities increases the stress concentration around the graphite nodules and can explain the initiation of multiple small cracks. In addition, the internal pressure build-up causes tensile stresses at the crack tips, which lead to locally increased hydrogen concentrations promoting the crack growth.

5 | CONCLUSIONS

Hydrogen thermal desorption from the DCI manifests two distinct peaks with maxima located between 400 and 500 K and close to 600 K at the heating rate of 10 K/min. The trapping energy for these peaks was found to be

0.30 ± 0.006 and 0.65 ± 0.03 eV, respectively. The low-temperature peak corresponds to hydrogen trapped at small cracks/voids forming at the interfaces of graphite nodules and ferrite matrix, while the high-temperature peak originates from hydrogen trapped in the graphite nodules.

Micrographs of the cross-sections of the polished DCI specimens after free immersion in 0.1 N H₂SO₄ solution, after interrupted CLT under continuous hydrogen charging, and after hydrogen charging without loading show intensive small crack initiation at interfaces between the graphite nodules and the ferrite matrix already at the initial stage of hydrogen uptake. These results confirm the observations on the presence of hydrogen in the graphite nodules and at the graphite/ferrite matrix interfaces.

Hydrogen-induced formation of multiple small cracks at the graphite/ferrite matrix interfaces and their linkage causes the increased elongation of cast iron in CLT. The ferrite matrix cracks by brittle cleavage fracture mechanism in the presence of hydrogen.

ACKNOWLEDGMENTS

The authors wish to thank the Finnish KYT2022 project for funding the research, as well as Posiva Oy, Finland, for providing the representative test material.

CONFLICT OF INTERESTS

The authors declare that there are no conflict of interests.

ORCID

Patrik Sahiluoma  <http://orcid.org/0000-0002-3310-1874>

Antti Forsström  <http://orcid.org/0000-0002-4519-9602>

REFERENCES

- [1] H. Raiko, R. Sandström, H. Ryden, M. Johansson, *SKB Report TR-10-28*, Stockholm, Sweden **2010**.
- [2] SKB, *SKB Report TR-16-15*, Stockholm, Sweden **2016**.
- [3] M. Jonsson, G. Emilsson, L. Emilsson, *Posiva SKB Report 04*, Eurajoki, Finland **2018**.
- [4] A. Forsström, Y. Yagodzinskyy, H. Hänninen, *Corros. Rev.* **2019**, *37*, 441.
- [5] M. Kolesnik, T. Aliev, V. Likhanskii, *J. Nucl. Mater.* **2018**, *508*, 567.
- [6] A. Mourujärvi, K. Widell, T. Saukkonen, H. Hänninen, *Fatigue Fract. Eng. Mater. Struct.* **2009**, *32*, 379.
- [7] K. Wallin, *Int. J. Metalcast.* **2014**, *8*, 81.
- [8] G. Hutter, L. Zybell, M. Kuna, *Eng. Fract. Mech.* **2015**, *144*, 118.
- [9] T. Takai, Y. Chiba, K. Noguchi, A. Nozue, *Metall. Mater. Trans. A* **2002**, *33*, 2659.
- [10] R. Wu, J. Ahlström, H. Magnusson, K. Frisk, Å. Martinsson, *SKB Report R-13-45*, Stockholm, Sweden **2015**.

- [11] H. Matsunaga, T. Usuda, K. Yanase, M. Endo, *Metall. Mater. Trans. A* **2014**, *45*, 1315.
- [12] T. Matsuo, *J. Phys.: Conf. Ser.* **2017**, *843*, 012012.
- [13] W. Y. Choo, J. Y. Lee, *Metall. Trans. A* **1982**, *13*, 135.
- [14] H. E. Kissinger, *Anal. Chem.* **1957**, *29*, 1702.
- [15] C. Zapffe, C. Sims, *Trans. Am. Inst. Min., Metall. Eng.* **1941**, *145*, 225.

How to cite this article: Sahiluoma P, Yagodzinskyy Y, Forsström A, Hänninen H, Bossuyt S. Hydrogen embrittlement of nodular cast iron. *Materials and Corrosion*. 2020;1–10.
<https://doi.org/10.1002/maco.202011682>